Communications

Spatiotemporal QRST Cancellation Techniques for Analysis of Atrial Fibrillation

Martin Stridh and Leif Sörnmo*

***Abstract*—A new method for QRST cancellation is presented for the analysis of atrial fibrillation in the surface electrocardiogram (ECG). The method is based on a spatiotemporal signal model which accounts for dynamic changes in QRS morphology caused, e.g., by variations in the electrical axis of the heart. Using simulated atrial fibrillation signals added to normal ECGs, the results show that the spatiotemporal method performs considerably better than does straightforward average beat subtraction (ABS). In comparison to the ABS method, the average QRST-related error was reduced to 58 percent. The results obtained from ECGs with atrial fibrillation agreed very well with those from simulated fibrillation signals.**

***Index Terms*—Atrial fibrillation, ECG, least squares estimation, QRS cancellation.**

I. Introduction

Atrial fibrillation (AF) is the most common sustained cardiac arrhythmia and afflicts as many as 10% of those over age 75 [1]. In contrast to the normal sinus rhythm, at which a single electrical activation wavefront propagates within the atria toward the ventricles, atrial fibrillation is manifested by the presence of multiple wandering wavefronts with different propagation patterns [2]. However, the exact mechanisms behind AF remains uncertain. Invasive mapping techniques have recently suggested that an atrial cycle length (ACL) can be measured as the time interval between consecutive activations in each measurement point [3].

In the surface electrocardiogram (ECG), atrial fibrillation is characterized by a fluctuating baseline which occurs in place of the P waves. The amplitude, shape, and regularity of this pattern vary substantially between different subjects; the pattern is in some cases regular and sawtooth-shaped while it is less regular and with lower amplitude in others. The characterization of AF is facilitated by a signal in which the ventricular activity, the QRST complex, has first been cancelled. The average beat subtraction (ABS) approach makes use of the fact that AF is uncoupled to ventricular activity and, therefore, the average beat is subtracted to produce a residual signal which contains the fibrillation waveforms [4]–[6]. The use of adaptive recurrent filtering is another related technique which has been considered for QRST cancellation. The impulse response of the filter is adapted to successive beats and then used for subtraction [7]; it was recently shown that this approach is identical to exponential averaging [8].

The above QRST cancellation methods rely on the assumption that the average beat can represent each individual beat accurately. However, QRS morphology is often subject to minor changes caused by variations in the electrical axis of the heart. These variations are primarily due to respiratory activity: the electrical axis of the QRS complex can during inspiration vary as much as 10° in the transversal plane and, accordingly, influences the precordial leads [9]. The lead V_2 is, in general, more sensitive to changes in position and orientation of the heart than the other precordial leads [10]. Due to the single-lead nature of the ABS method, axis variations can sometimes cause considerable QRS-related errors. Since these variations may occur on a beat-to-beat basis, exponential averaging cannot handle this problem in a satisfactory way.

A new technique for vectorcardiographic loop alignment was recently introduced for the purpose of separating morphologic beat-to-beat variability from respiratory-induced variations [11], [12]. In this paper, the alignment technique is generalized to perform QRST cancellation and introduces multilead information in the *cancellation* process (Section II). The resulting residual signal constitutes the basis for subsequent time-frequency analysis of atrial fibrillation, a topic which is considered in [13]. The performance of the new QRST cancellation technique is studied both by means of a simulation model for atrial fibrillation and a set of ECG signals and is compared to that of the ABS method (Sections III, IV and V).

II. Methods

A. Observation Model

Each cardiac cycle in the ECG is assumed to be represented by an $N\times L$ matrix $\mathbf{Y}$ which contains N samples from L leads

$$\mathbf{Y} = [\mathbf{y}_1 \quad \cdots \quad \mathbf{y}_L] \tag{1}$$

where the vector $\mathbf{y}_l$ contains the samples of the lth lead. The atrial fibrillation is viewed as being uncoupled to the ventricular activity and, thus, each observed beat is modeled as a sum of atrial activity ($\mathbf{Y}_A$), ventricular activity ($\mathbf{Y}_V$), and additive noise ($\mathbf{W}'$)

$$\mathbf{Y} = \mathbf{Y}_A + \mathbf{Y}_V + \mathbf{W}'. \tag{2}$$

An averaged beat $\mathbf{X}$ ($(N+2\Delta)\times L$) is used to represent the ventricular activity. A spatial alignment matrix $\mathbf{S}$ ($L\times L$) is defined which introduces the following properties in the cancellation process:

- possibility to shift information between the leads to compensate for variations in the electrical axis;
- scaling to compensate for variations in tissue conductivity and heart position, possibly affecting the amplitude in different leads.

The matrix $\mathbf{S}$ is defined as the product of a diagonal amplitude scaling matrix $\mathbf{D}$ and a rotation matrix $\mathbf{Q}$, i.e.,

$$\mathbf{S} = \mathbf{D}\mathbf{Q} \tag{3}$$

where the diagonal elements d_l in $\mathbf{D}$ are positive-valued.[1]

Furthermore, a time shift matrix $\mathbf{J}_\tau$ is introduced which corrects for misalignment in time between the observed and the averaged beat. The time shift matrix is defined by

$$\mathbf{J}_\tau = \begin{bmatrix}\mathbf{0}_{N\times(\Delta+\tau)} & \mathbf{I}_{N\times N} & \mathbf{0}_{N\times(\Delta-\tau)}\end{bmatrix} \tag{4}$$

[1]It should be noted that the present definition of $\mathbf{D}$ is more general than that previously described in [11] where $\mathbf{D} = \alpha\mathbf{I}$ (α is a scalar and $\mathbf{I}$ is the identity matrix).

Manuscript received June 18, 1999; revised September 1, 2000. This work was supported by the Swedish National Board for Technical Development (NUTEK). *Asterisk indicates corresponding author.*

M. Stridh is with the Signal Processing Group, Department Applied Electronics, Lund University, S-221 00 Lund, Sweden.

*L. Sörnmo is with the Signal Processing Group, Department Applied Electronics, Lund University, Box 118, S-221 00 Lund, Sweden (e-mail: leif.sornmo@tde.lth.se).

Publisher Item Identifier S 0018-9294(01)00140-9.

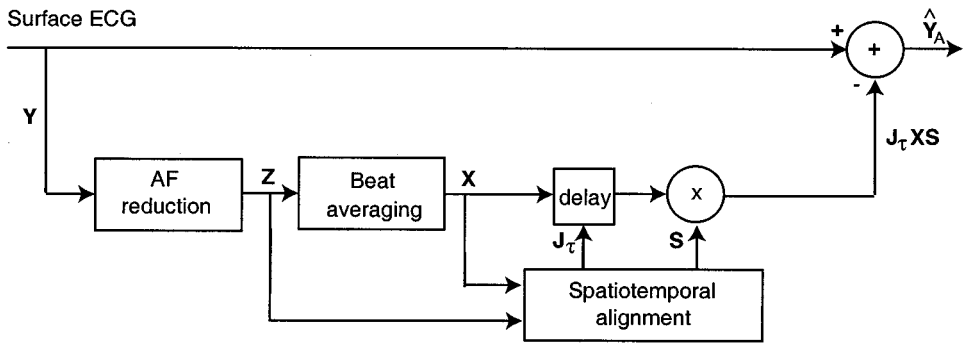

Fig. 1. Spatiotemporal QRST cancellation. The fibrillation is extracted from the ECG by subtracting an aligned average beat. An intermediate signal $\mathbf{Z}$ is used for reducing the AF influence in the cancellation process.

and selects those N samples of the averaged beat that provide the best fit to the observed beat $\mathbf{Y}$. The maximum time synchronization error that can be corrected is equal to $\pm\Delta$. Thus, the ventricular activity is modeled by

$$\mathbf{Y}_V = \mathbf{J}_\tau \mathbf{X}\mathbf{S}. \tag{5}$$

Ultimately, the aim is to first find estimates of the parameters $\mathbf{Q}$, $\mathbf{D}$ and τ and then to subtract the resulting estimate of $\mathbf{Y}_V$ from $\mathbf{Y}$. By combining (2) and (5) we get

$$\mathbf{Y} - \mathbf{J}_\tau \mathbf{X}\mathbf{S} = \mathbf{W}' + \mathbf{Y}_A. \tag{6}$$

It is obvious from the right-hand side of (6) that not only the noise $\mathbf{W}'$ will limit how well $\mathbf{J}_\tau\mathbf{X}\mathbf{S}$ fits $\mathbf{Y}$ but the atrial activity $\mathbf{Y}_A$ as well. In order to handle this problem, we introduce an intermediate estimate $\hat{\mathbf{Y}}_A$ to be subtracted from the observed signal prior to the estimation of the cancellation parameters

$$\mathbf{Z} - \mathbf{J}_\tau \mathbf{X}\mathbf{S} = \mathbf{W}' + \mathbf{Y}_A - \hat{\mathbf{Y}}_A = \mathbf{W} \tag{7}$$

where

$$\mathbf{Z} = \mathbf{Y} - \hat{\mathbf{Y}}_A. \tag{8}$$

The process of subtracting $\hat{\mathbf{Y}}_A$ in (7) is referred to as *AF reduction*; the actual method used for computing the intermediate estimate is described in Section II-C.

B. Estimation of QRST Cancellation Parameters

The QRST cancellation parameters $\mathbf{Q}$, $\mathbf{D}$, and τ are estimated by solving the following minimization problem

$$\epsilon^2_{\min} = \min_{\mathbf{D},\mathbf{Q},\tau} \|\mathbf{Z} - \mathbf{J}_\tau \mathbf{X}\mathbf{D}\mathbf{Q}\|_F^2 \tag{9}$$

where the Frobenius norm for an arbitrary matrix $\mathbf{A}$ is defined by $\|\mathbf{A}\|_F^2 = \mathrm{tr}(\mathbf{A}\mathbf{A}^T)$. Minimization with respect to $\mathbf{Q}$ and $\mathbf{D}$ cannot be done independently and a closed-form solution is difficult to find. An alternating, iterative approach is, therefore, used in which the error

$$\epsilon^2 = \mathrm{tr}(\mathbf{Z}\mathbf{Z}^T) + \mathrm{tr}\left(\mathbf{J}_\tau\mathbf{X}\mathbf{D}\mathbf{D}^T\mathbf{X}^T\mathbf{J}_\tau^T\right) - 2\,\mathrm{tr}\left(\mathbf{D}^T\mathbf{X}^T\mathbf{J}_\tau^T\mathbf{Z}\mathbf{Q}^T\right) \tag{10}$$

can be minimized with respect to $\mathbf{Q}$ by maximizing the last term under the assumption that $\mathbf{D}$ is known. The maximization is performed by using singular value decomposition (SVD) [14]. In general, the SVD decomposes a matrix $\mathbf{T}$ into two orthonormal matrices, $\mathbf{U}$ and $\mathbf{V}$, and a diagonal matrix $\mathbf{\Sigma}$ that contains the singular values σ_l

$$\mathbf{T} = \mathbf{U}\mathbf{\Sigma}\mathbf{V}^T. \tag{11}$$

By setting $\mathbf{T} = \mathbf{D}^T\mathbf{X}^T\mathbf{J}_\tau^T\mathbf{Z}$, the last term in (10) can be expressed as $2\,\mathrm{tr}(\mathbf{T}\mathbf{Q}^T)$ which is maximized for [14]

$$\hat{\mathbf{Q}} = \mathbf{U}\mathbf{V}^T. \tag{12}$$

After estimating $\mathbf{Q}$, (10) can be written

$$\epsilon^2 = \mathrm{tr}[(\mathbf{Z}\mathbf{Q}^{-1} - \mathbf{J}_\tau\mathbf{X}\mathbf{D})\mathbf{Q}\mathbf{Q}^T(\mathbf{Z}\mathbf{Q}^{-1} - \mathbf{J}_\tau\mathbf{X}\mathbf{D})^T] \tag{13}$$

where the introduction of $\mathbf{Z}' = \mathbf{Z}\mathbf{Q}^{-1}$ yields

$$\epsilon^2 = \mathrm{tr}[(\mathbf{Z}' - \mathbf{J}_\tau\mathbf{X}\mathbf{D})(\mathbf{Z}' - \mathbf{J}_\tau\mathbf{X}\mathbf{D})^T]. \tag{14}$$

Equation (14) can be rearranged as

$$\epsilon^2 = \mathrm{tr}(\mathbf{Z}'\mathbf{Z}'^T) + \mathrm{tr}\left(\mathbf{D}\mathbf{D}^T\mathbf{X}^T\mathbf{J}_\tau^T\mathbf{J}_\tau\mathbf{X}\right) - 2\,\mathrm{tr}\left(\mathbf{D}^T\mathbf{X}^T\mathbf{J}_\tau^T\mathbf{Z}'\right) \tag{15}$$

and is, since $\mathbf{D}$ is a diagonal matrix, minimized by setting the derivative with respect to the diagonal entries of $\mathbf{D}$ equal to zero. For a given $\mathbf{Q}$, the diagonal entries in $\mathbf{D}$ can be estimated by

$$\hat{d}_l = \left([\mathbf{J}_\tau\mathbf{X}]_l^T[\mathbf{J}_\tau\mathbf{X}]_l\right)^{-1}\left([\mathbf{J}_\tau\mathbf{X}]_l^T[\mathbf{Z}']_l\right), \quad l = 1,\ldots,L. \tag{16}$$

An improved estimate of $\mathbf{Q}$ is then estimated based on the new scale factor estimate $\hat{d}_l$.

Typically, a solution close to $\mathbf{Q} = \mathbf{D} = \mathbf{I}$ is desirable and, therefore, the algorithm is initialized with $\mathbf{D}_0 = \mathbf{I}$ (the ABS method, thus, serves as the starting point for the spatiotemporal method). The rotation at step k, $\mathbf{Q}_k$, is then calculated from $\mathbf{D}_{k-1}$. Since

$$\|\mathbf{Z} - \mathbf{J}_\tau\mathbf{X}\mathbf{D}_{k-1}\mathbf{Q}_k\|_F \le \|\mathbf{Z} - \mathbf{J}_\tau\mathbf{X}\mathbf{D}_{k-1}\mathbf{Q}_{k-1}\|_F \tag{17}$$

the error will be less or equal to that in the previous step. When $\mathbf{Q}_k$ is known, $\mathbf{D}_k$ can be calculated. Accordingly

$$\|\mathbf{Z} - \mathbf{J}_\tau\mathbf{X}\mathbf{D}_k\mathbf{Q}_k\|_F \le \|\mathbf{Z} - \mathbf{J}_\tau\mathbf{X}\mathbf{D}_{k-1}\mathbf{Q}_k\|_F. \tag{18}$$

This procedure is repeated until the difference in error between two successive iterations is sufficiently small. The algorithm will converge since the minimization with regard to both $\mathbf{Q}$ and $\mathbf{D}$ for each step according to (17) and (18) will improve the fit in terms of ϵ^2 [15].

Finally, the minimization with respect to τ is solved by a grid search of τ in the interval $[-\Delta, \Delta]$; estimates of $\mathbf{Q}$ and $\mathbf{D}$ must obviously be computed for all values of τ. The block diagram in Fig. 1 summarizes the different steps of the spatiotemporal QRST cancellation method.

C. TQ-Based Fibrillation Signal

The model parameter estimation is hampered by the presence of AF. In order to reduce the influence of AF, an intermediate fibrillation signal, $\hat{\mathbf{Y}}_A$, is reconstructed during the QRST interval from the adjacent TQ intervals and subtracted from each observed beat prior to estimation. A simple approach is used in which the fibrillation cycle prior to the QRST complex is replicated during the QRST interval but linearly weighted such that the weights decrease from one at the onset of the interval to zero at the end. An identical procedure is applied to the fibrillation cycle following the QRST complex but in a time-reversed fashion. The TQ-based fibrillation signal is obtained by summing the two replicated waveforms. The length of the fibrillation cycle to be replicated is estimated from the autocorrelation function of the two adjacent QT intervals. The TQ-based fibrillation signal is set to zero whenever both the adjacent RR intervals are too short. If only one of the RR intervals is sufficiently long, that interval is used for reconstructing the signal. The TQ-based fibrillation signal is constructed for each individual lead to allow for lead-dependent AF properties.

It should be emphasized that the AF reduction improves the accuracy of the model parameter estimates while not directly influencing the atrial activity in the ECG.

D. Average Beat Subtraction

The ABS method uses the conventional, arithmetic average for subtraction of the ventricular activity. The ABS method can be viewed as a special case of (5) in which no spatial alignment is performed, i.e., $\mathbf{S} = \mathbf{I}$

$$\mathbf{Y}_V = \mathbf{J}_\tau \mathbf{X} \tag{19}$$

and, thus, the time delay, τ, is the only parameter to be estimated.

The ABS method is made identical to that in [4] by using the observed beat $\mathbf{Y}$ instead of the AF reduced beat $\mathbf{Z}$. It is likely that differences in performance when using $\mathbf{Z}$ instead of $\mathbf{Y}$ are negligible since the spatial alignment is omitted. The ABS minimization problem is defined by

$$\epsilon^2_{\min} = \min_\tau \|\mathbf{Y} - \mathbf{J}_\tau \mathbf{X}\|^2_F \tag{20}$$

and is done by a grid search over all admissible values of τ.

III. Simulation Model and Database

In order to study performance, we have employed simulated as well as recorded ECG data. The test signals were generated by adding simulated AF signals to ECG signals obtained from healthy subjects. The main advantage of taking the ventricular activity from healthy subjects is that inherent variations in QRS morphology are present.

A. ECG Database

The simulation study was based on ECGs from 15 healthy subjects (see [16] for further details) which were acquired at a sampling rate of 1 kHz. The cancellation technique was also tested on ECGs from 20 subjects suffering from chronic atrial fibrillation using leads V_1, V_2 and V_3.

Linear-phase, highpass filtering (cut-off frequency at 0.3 Hz) was used to reduce baseline wander before performing QRST cancellation. Crosscorrelation-based beat classification was performed so that beats with different morphologies were separated into different classes [16]. A beat average was then computed for each of the classes. Although a class sometimes contained only one, or a few beats, the corresponding beat average was still used for cancellation. It should be noted that a class containing one single beat cancels itself completely including the AF.

TABLE I
Parameter Values Defining the Simulated Fibrillation Patterns A and B

Parameter	case A	case B
Frequency, f_0	6 Hz	8 Hz
Frequency variation, Δf	0.2 Hz	0.3 Hz
Frequency variation frequency, f_f	0.1 Hz	0.23 Hz
Harmonics, M	5	3
Amplitude, a_l [V_1 V_2 V_3]	[150 75 45] μV	[60 50 40] μV
Amplitude variation, Δa_l [V_1 V_2 V_3]	[50 25 15] μV	[18 15 12] μV
Amplitude variation frequency, ω_a	0.08 Hz	0.5 Hz

The onset of the averaged beat $\mathbf{X}$ differed between the two groups: for normals, the onset was taken 200 ms prior to the Q wave to ensure cancellation of the P waves while, for AF patients, the onset was identical to the Q wave onset. The model parameters were, in all cases, estimated from the QRS interval.

B. Simulation of Atrial Fibrillation

The dynamics of the simulated AF are defined such that the resulting signal mimics AF in the ECG. A sinusoid and $M-1$ harmonics are used to generate the sawtooth-similar shape of AF. The nonstationary behavior is created by introducing a time-varying amplitude and cycle length of the sawtooth signal. The atrial activity in the lth lead is modeled by

$$y_l(n) = -\sum_{i=1}^{M} a_{l,i}(n)\sin(i\theta(n)), \quad n = 1, \ldots, N \tag{21}$$

where $a_{l,i}(n)$ for sawtooth amplitude, a_l, modulation peak amplitude, Δa_l, and amplitude modulation frequency, f_a, is given by

$$a_{l,i}(n) = \frac{2}{i\pi}\left(a_l + \Delta a_l \sin 2\pi \frac{f_a}{F_s} n\right). \tag{22}$$

The fundamental of the fibrillation waveform is assumed to vary around the frequency f_0 with a maximum frequency deviation of Δf and modulation frequency given by f_f. The phase, $\theta(n)$, is then given by [17]

$$\theta(n) = 2\pi \frac{f_0}{F_s} n + \left(\frac{\Delta f}{f_f}\right) \sin 2\pi \frac{f_f}{F_s} n. \tag{23}$$

Two fibrillatory patterns are considered for performance evaluation:

- rather long cycle lengths, large amplitude and several harmonics (case A);
- less sharp waveforms with shorter cycle length and low amplitude (case B).

The setup of parameter values that define each of these two types of fibrillation is presented in Table I and the case A signals are exemplified in Fig. 2.

IV. Performance Measures

The fact that the AF activity is known in the simulated ECGs allows us to do an in-depth study of the QRST cancellation performance. The performance measure is designed to reflect large QRS-related errors as well as errors due to that the electrical axis is not constant throughout the entire cardiac cycle and, therefore, T wave-related errors are introduced. These errors are described by a measure, M, which for each beat is defined by

$$M = \frac{1}{N}\|\mathbf{Y}_A - \hat{\mathbf{Y}}_A\|^2_F - \hat{\sigma}^2 \tag{24}$$

where $\hat{\sigma}^2$ is the sum of the estimated noise variances in the different leads, $\hat{\sigma}^2 = \sum_l \hat{\sigma}^2_l$. The noise variance $\hat{\sigma}^2_l$ in lead l is estimated from

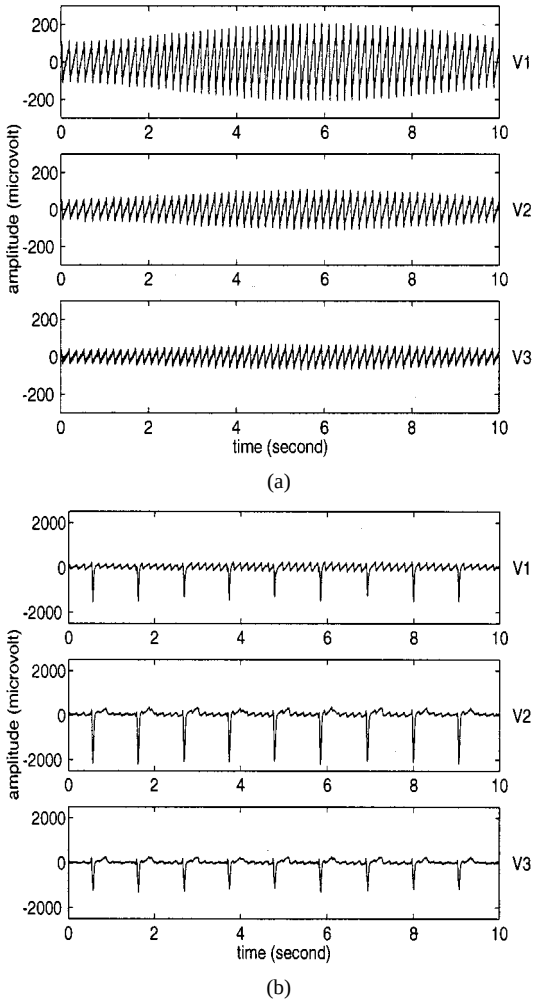

Fig. 2. The simulated fibrillation signals (leads V_1–V_3). (a) Case A fibrillation with relatively long cycle length and large amplitude. (b) The simulated fibrillation pattern superimposed on a normal ECG.

the entire ensemble of time-aligned beats in the recording before adding the simulated fibrillation signals [18]. The reason for compensating M with $\hat{\sigma}^2$ is to correct for the error that is due to noise in the ECG. The measure $\bar{M}$ is an average of all M values for the beats in a recording.

We define also two related performance measures, $\bar{M}_{\mathrm{QRS}}$ and $\bar{M}_{\overline{\mathrm{QRS}}}$, which describe the averaged error within and outside, respectively, of the alignment interval.

V. Results

A. Simulated Signals

1) Comparison Between Spatiotemporal Cancellation and Average Beat Subtraction: The performance of the spatiotemporal cancellation method was investigated in terms of a normalized mismatch error: $\bar{M}$ was always set to one for the ABS method. The only design parameters are the maximum synchronization in time, Δ, which was set to 5 ms and the maximum number of QD iterations which was set to ten. The results in Table II show that the spatiotemporal cancellation method performs considerably better than does the ABS method. For case A fibrillation, superior performance is achieved by the spatiotemporal cancellation method since the mismatch error is significantly reduced in all subjects: the mean error is only 58% of that for the ABS method. It should be emphasized that this value represent the error during the entire cardiac cycle while the parameter estimation is based on the QRS interval only.

TABLE II
Error Reduction Factors Based on the Entire Cardiac Cycle

	case A		case B	
Method	*Mean*	*Std*	*Mean*	*Std*
entire beat	0.58	0.15	0.62	0.18
QRS	0.28	0.15	0.31	0.12
outside QRS	1.12	0.25	1.10	0.24

TABLE III
Unnormalized, Average Error Amplitude Per Sample for V_1, V_2 and V_3 Combined

Interval	*Averaged* $\bar{M}$	*change*
entire beat	560.2	-40%
QRS	3392.2	-70%
outside QRS	220.2	+11%

Furthermore, Table II shows that the performance of the spatiotemporal cancellation is essentially the same for case B fibrillation having a more rapid variation in amplitude and frequency.

The errors related to the alignment interval ($\bar{M}_{\mathrm{QRS}}$) and to the interval outside the alignment interval ($\bar{M}_{\overline{\mathrm{QRS}}}$) are also presented in Table II. For both types of fibrillation, the QRS-related errors are dramatically reduced to about 30%. When compared to the results for the entire cardiac cycle it is clear that if the reduction is better within the alignment interval it cannot be equally good outside. However, we note that since the beat is often several times longer than the alignment interval and that no reduction can be expected outside the alignment interval, $\bar{M}_{\overline{\mathrm{QRS}}}$ should be close to one. The performance outside the alignment interval gets about 10% worse which, since the error already is low outside the alignment interval, in most cases is close to the inherent noise level of the ECG. Table III presents the unnormalized values of $\bar{M}$, $\bar{M}_{\mathrm{QRS}}$, $\bar{M}_{\overline{\mathrm{QRS}}}$ as averaged over all recordings in the database. From this table it can be concluded that the 11% decrease in performance outside the alignment interval is negligible when compared to the error reduction to 30% obtained during the QRS complex since the errors when using average beat subtraction in average are 15 times larger during the QRS complexes than outside (compare 3392 and 220).

We will now present some examples which demonstrate the performance of the spatiotemporal cancellation. The residual ECG and the error signal, i.e., the difference between the residual ECG and the simulated AF, as produced by the two methods, are shown in Fig. 3. Comparing the error signals in Fig. 3(c) and (d), it is obvious that the spatiotemporal method results in a better QRS cancellation than does the ABS method. It may be of interest to point out the small errors occurring during the T wave interval which are due to rapidly varying T wave morphology, see Fig. 3(c) and (d). This limitation in cancellation performance is similar for both methods.

The performance measures are based on an error signal such as the one shown in Fig. 3(c) and (d). This error signal contains, however, not only deviations between the estimated and the generated fibrillation signal but deviations due to inherent ECG noise as well. The M values in Table II are based on this error signal and then corrected with the ensemble noise variance, as described by (24). The example in Fig. 3 corresponds to an over-all reduction to 35% of disturbances related to ventricular activity.

2) Model Parameter Trends: Additional insight into the cancellation process is provided by studying the entries of the spatial alignment matrix $\mathbf{S}$ as a function of time. The diagrams in Fig. 4 show how the diagonal entries evolve with time (values are close to one). The off-diagonal entries are also plotted and indicate to what extent the other two

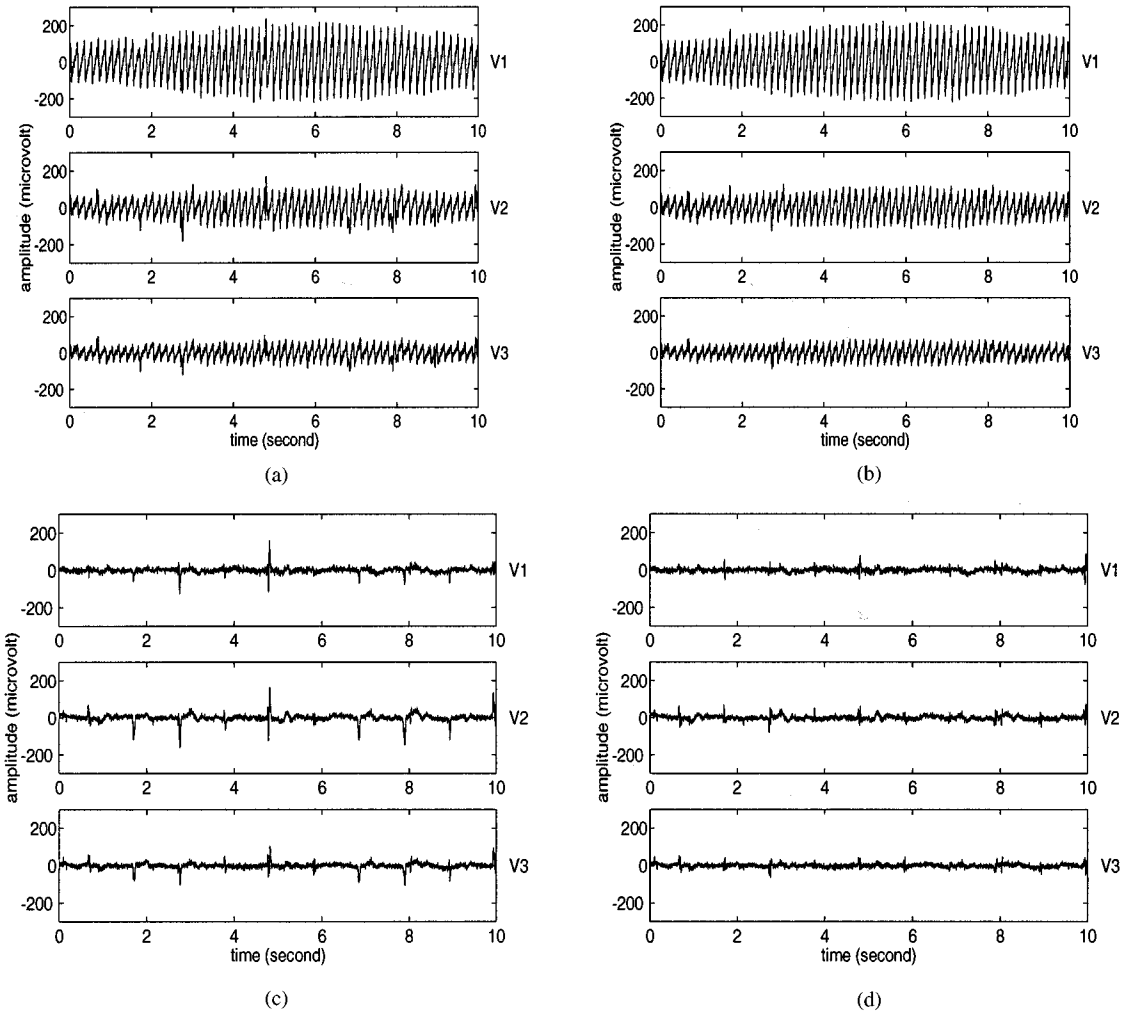

Fig. 3. Performance comparison: residual ECG obtained by (a) the ABS and (b) the spatiotemporal method and the corresponding error signal for (c) the ABS and (d) the spatiotemporal method.

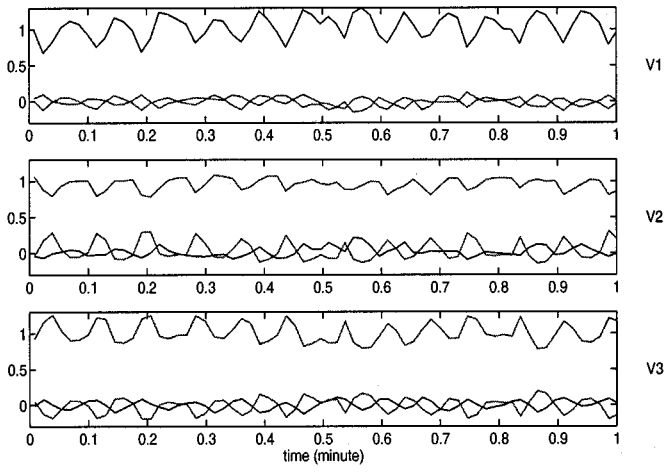

Fig. 4. Matrix entries of $\mathbf{S}$ as a function of time (see text for details).

leads are used for cancellation (values are close to zero). The oscillatory pattern, which is more or less apparent in all entries of $\mathbf{S}$, is most likely related to respiratory activity; the rate can be approximately estimated to 12 breaths per minute. A similar observation can be made from the error signal shown in Fig. 5 where a considerable QRS-related periodic variation remains after processing with the ABS method while the variation is removed by the spatiotemporal method. Thus, the degree of freedom introduced by $\mathbf{S}$ for combining leads can compensate for variations in the electrical axis of the heart.

B. ECG Data with Atrial Fibrillation

In order to support the above results based on simulated signals, we present a representative example taken from a patient with chronic atrial fibrillation where the performance of the method resembles that for the simulated signals, see Fig. 6. The QRS-related errors are substantially reduced using spatiotemporal cancellation in Fig. 6 and the improvement is most obvious in leads with weak AF, in this case V_2 and V_3. This property makes the spatiotemporal method well-suited, e.g., for use in conjunction with spectral analysis (see [13]).

VI. Discussion

The spatial matrix $\mathbf{S}$ is the product of a scaling matrix $\mathbf{D}$ and a rotation matrix $\mathbf{Q}$. The scaling matrix plays an important role to emphasize or deemphasize information in the different leads. Although rotation lacks an intuitive, geometrical interpretation when nonorthogonal leads are used, variations in the electrical axis of the heart still appear to be well represented by the entries of the rotation matrix.

The convergence of the alternating, iterative estimation procedure for $\mathbf{D}$ and $\mathbf{Q}$ was studied in terms of average squared error for all beats.

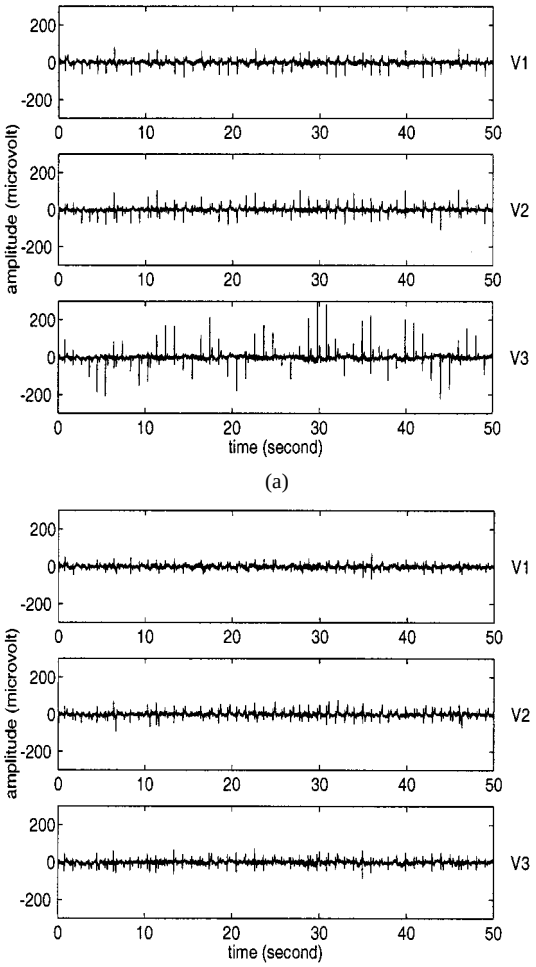

Fig. 5. Residual ECG from which the known fibrillation signal has been subtracted by (a) the ABS method and (b) the spatiotemporal cancellation method.

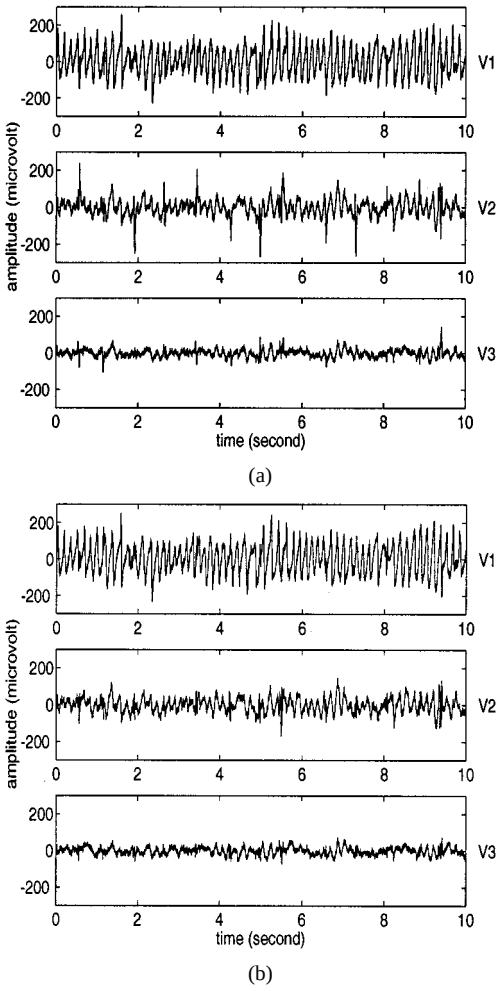

Fig. 6. Residual ECG: (a) average beat subtraction; (b) spatiotemporal cancellation.

In almost all recordings, the major improvement was obtained already after one iteration, however, further iterations sometimes reduced ϵ^2 to a minor degree. It is difficult to present exact figures on the improvement associated with further iterations since part of the remaining error is due to inherent ECG noise.

It was shown that the improvement in QRS cancellation was coupled to a slight performance reduction during the T wave interval. Such a reduction can actually be expected since the ventricular rhythm is highly irregular during AF and, accordingly, it becomes more difficult to cancel the T wave when its duration varies from cycle to cycle. Nevertheless, the results suggest that the inclusion of, e.g., a two-step procedure for QRS and T cancellation is not warranted, especially when considering the difficulties associated with delineation of the QRS complex and the T wave in the presence of AF.

The AF reduction, performed prior to parameter estimation, turned out to be crucial for efficient QRST cancellation. A simple and fast method was considered in which the fibrillatory waves in the adjacent TQ intervals are used to produce an intermediate AF signal. In our experience, the exact design of the AF reduction method is less critical and requires that the signal has approximately correct cycle length and amplitude. In general, low amplitude AF possesses a less well-defined cycle length and is, therefore, more difficult to use for computation of an intermediate signal. Fortunately, the influence of such AF in the cancellation process is less significant. On the other hand, large amplitude AF tends to be more "organized" with an obvious cycle length and is, therefore, better suited for successful AF reduction. In the present study, these observations are supported by the results obtained for the simulated fibrillation signals: it is easier to reconstruct case A fibrillation than case B because of its slower variations in amplitude and frequency.

Other structures of the spatial matrix $\mathbf{S}$ have been investigated elsewhere [19], notably one with a global scaling parameter ($\mathbf{S} = \alpha\mathbf{Q}$) and another with a linear mapping matrix without any constraints ($\mathbf{S} = \mathbf{P}$). The $\alpha\mathbf{Q}$ method resulted in a reduction of the error to 66% of that for ABS but still performed worse than when using the definition in (3) of $\mathbf{S}$. The $\mathbf{P}$-based cancellation method did not yield any improvement at all over the ABS method and, thus, it is concluded that a too large degree of freedom reduces the robustness of the QRST cancellation.

ACKNOWLEDGMENT

The authors would like to thank Prof. B. Olsson and Dr. M. Holm of the Department of Cardiology, Lund University, for initiating this study and for providing several valuable comments.

REFERENCES

[1] N. M. Wheeldon, "Atrial fibrillation and anticoagulant therapy," *Eur. Heart J.*, vol. 16, pp. 302–312, 1995.

[2] M. Allessie, K. Konings, and M. Wijffels, *Atrial Arrhythmias—State of the Art: Electrophysiological Mechanism of Atrial Fibrillation*, J. P. DiMarco and E. N. Prystowsky, Eds. Armonk, NY: Futura Publ. Co., 1995.

[3] M. Holm, R. Johansson, S. B. Olsson, J. Brandt, and C. Lührs, "A new method for analysis of atrial activation during chronic atrial fibrillation in man," *IEEE Trans. Biomed. Eng.*, vol. 43, pp. 198–210, Feb. 1996.
[4] J. Slocum, E. Byrom, L. McCarthy, A. Sahakian, and S. Swiryn, "Computer detection of atrioventricular dissociation from surface electrocardiograms during wide QRS complex tachycardia," *Circulation*, vol. 72, pp. 1028–1036, 1985.
[5] M. Holm, S. Pehrsson, M. Ingemansson, L. Sörnmo, R. Johansson, L. Sandhall, M. Sunemark, B. Smideberg, C. Olsson, and B. Olsson, "Non-invasive assessment of atrial refractoriness during atrial fibrillation in man—Introducing, validating and illustrating a new ECG method," *Cardiovasc. Res.*, vol. 38, pp. 69–81, 1998.
[6] S. Shkurovich, A. Sahakian, and S. Swiryn, "Detection of atrial activity from high-voltage leads of implantable ventricular defibrillators using a cancellation technique," *IEEE Trans. Biomed. Eng.*, vol. 45, pp. 229–234, Aug. 1998.
[7] N. Thakor and Y. Zhu, "Applications of adaptive filtering to ECG analysis: Noise cancellation and arrhythmia detection," *IEEE Trans. Biomed. Eng.*, vol. 38, pp. 785–793, Aug. 1991.
[8] P. Laguna, R. Jane, E. Masgrau, and P. Caminal, "The adaptive linear combiner with a periodic-impulse reference input as a linear comb filter," *Signal Proc.*, vol. 48, pp. 193–203, 1996.
[9] J. Malmivuo and R. Plonsey, *Bioelectromagnetism*. Oxford, U.K.: Oxford Univ. Press, 1995.
[10] G. J. M. Huiskamp and A. van Oosterom, "Heart position and orientation in forward and inverse electrocardiography," *Med. Biol. Eng. Comput.*, no. 30, pp. 613–620, 1992.
[11] L. Sörnmo, "Vectorcardiographic loop alignment and morphologic beat-to-beat variability," *IEEE Trans. Biomed. Eng.*, vol. 45, pp. 1401–1413, Dec. 1998.
[12] M. Åström, E. Carro, L. Sörnmo, P. Laguna, and B. Wohlfart, "Vectorcardiographic loop alignment and the measurement of morphologic beat-to-beat variability in noisy signals," *IEEE Trans. Biomed. Eng.*, vol. 46, pp. 497–506, Apr. 2000.
[13] M. Stridh, L. Sörnmo, C. Meurling, and B. Olsson, "Characterization of atrial fibrillation using the surface ECG: Spectral analysis and time-dependent properties," *IEEE Trans. Biomed. Eng.*, vol. 48, pp. 19–27, Jan. 2001.
[14] G. Golub and C. van Loan, *Matrix Computations*, 2nd ed. Baltimore, MD: The Johns Hopkins Univ. Press, 1989.
[15] M. Koschat and D. Swayne, "A weighted Procrustes criterion," *Psychometrica*, vol. 56, no. 2, pp. 229–239, 1991.
[16] L. Sörnmo, B. Wohlfart, J. Berg, and O. Pahlm, "Beat-to-beat QRS variability in the 12-lead ECG and the detection of coronary heart disease," *J. Electrocardiol.*, vol. 31, pp. 336–344, 1998.
[17] P. Young, *Electronic Communication Techniques*, 3rd ed. Columbus, OH: Merrill, 1994.
[18] E. Berbari, L. DeCarlo, B. Scherlag, and R. Lazzara, "Optimizing the signal averaging method for ventricular late potentials," in *Proc. Computers in Cardiology*, 1984, pp. 45–49.
[19] M. Stridh and L. Sörnmo. (1998) Spatiotemporal QRST cancellation techniques for atrial fibrillation analysis in the surface ECG. SPR 44 Lund Univ., Lund, Sweden. [Online]. Available: http://www.tde.lth.se/research/sig/Sigreport.html

Automatic Differentiation of Multichannel EEG Signals

B. O. Peters, G. Pfurtscheller, and H. Flyvbjerg*

***Abstract*—Intention of movement of left or right index finger, or right foot is recognized in electroencephalograms (EEGs) from three subjects. We present a multichannel classification method that uses a "committee" of artificial neural networks to do this. The classification method *automatically* finds spatial regions on the skull relevant for the classification task. Depending on subject, correct recognition of intended movement was achieved in 75%–98% of trials not seen previously by the committee, on the basis of single EEGs of one-second duration. Frequency filtering did not improve recognition. Classification was optimal during the actual movement, but a first peak in the classification success rate was observed in all subjects already when they had been cued which movement later to perform.**

***Index Terms*—Artificial neural nets, autoregressive modeling, brain-computer interface, multichannel time series analysis.**

I. Introduction

It has long been known that human electroencephalogram (EEG) activity is altered before, during, and after sensory-motor processing and other mental activities. It has also been known for some time that EEGs produced during a very limited set of mental tasks can be classified, hence recognized, according to tasks [1]–[7]. A classifier doing this can then be used to control a device by having each task correspond to a command. This concept is referred to as a *brain-computer interface* (BCI). For such applications, speed and reliability of recognition matter. A purely academical interest in the information content in EEG takes a similar interest in its dependence on the duration of the signal, circumstances of recording, and enhancement by filtering.

In this paper, we present a method that automatically finds relevant EEG channels, and classifies as well or better than other schemes. Our method was developed on data presented and studied first in [4]. These data were recorded on three subjects before, during, and after movements of right foot, left index finger, and right index finger.

Section II describes the EEG experiment. Section III describes our preprocessing, feature extraction, and classification scheme. Section IV describes our filter settings and the time course of classification of three types of movement for various frequency bands and spatial regions on the skull. In Section V, we compare our classification rates to results obtained by other groups.

II. Experimental Setup

The test subjects' EEG potentials were measured on 56 silver/silver-chloride electrodes with a reference electrode on the nose-tip. The electrodes were positioned on a rectangular grid with an approximate spacing between neighboring electrodes of 2.5 cm. Four electrodes corresponded to the international 10–20 system [8], see Fig. 1. The sampling rate, f_s, was 128 Hz, giving $56 \times 128 = 7168$

Manuscript received July 2, 1999; revised September 9, 1999. This work was supported in part by the "Fonds zur Förderung der wissenschaftlichen Forschung" in Austria under Project P11208-MED. *Asterisk indicates corresponding author.*

B. O. Peters is with the John von Neumann Institute for Computing, Forschungszentrum Jülich, D-52425 Jülich, Germany.

G. Pfurtscheller is with the Institute of Biomedical Engineering, Department of Medical Informatics, Brockmanngasse 41, A-8010 Graz, Austria.

*H. Flyvbjerg is with the Condensed Matter Physics and Chemistry Department, Risø National Laboratory, PO Box 49, DK-4000 Roskilde, Denmark, and The Niels Bohr Institute, Blegdamsvej 17, DK-2100 Copenhagen Ø, Denmark (e-mail: H.Flyvbjerg@NBI.dk).

Publisher Item Identifier S 0018-9294(01)00141-0.